Supporting Information

Two-Photon Interference from the Far-Field Emission of Chip-Integrated Cavity-Coupled Emitters

Je-Hyung Kim,[†] *Christopher J. K. Richardson*,[‡] *Richard P. Leavitt*,[‡] *and Edo Waks**[,†,§]

[†]Department of Electrical and Computer Engineering and Institute for Research in Electronics and Applied Physics, University of Maryland, College Park, Maryland 20742, United States

[‡]Laboratory for Physical Sciences, University of Maryland, College Park, Maryland 20740, United States

[§]Joint Quantum Institute, University of Maryland and the National Institute of Standards and Technology, College Park, Maryland 20742 , United States

Corresponding Author

*E-mail: edowaks@umd.edu

Photoluminescence spectra of bulk dots and cavity-coupled dots

Figure S1a,b shows photoluminescence spectra of the cavity-coupled dot A in the manuscript and bulk dots outside photonic crystal region measured at the same pump power. The intensity of cavity-coupled dots is an order of magnitude higher than that for bulk dots. For the bulk dots a large difference in refractive index at the surface reflects most of emission from the air to InP surface, resulting in poor collection efficiency of less than 1% at the first lens.[1]

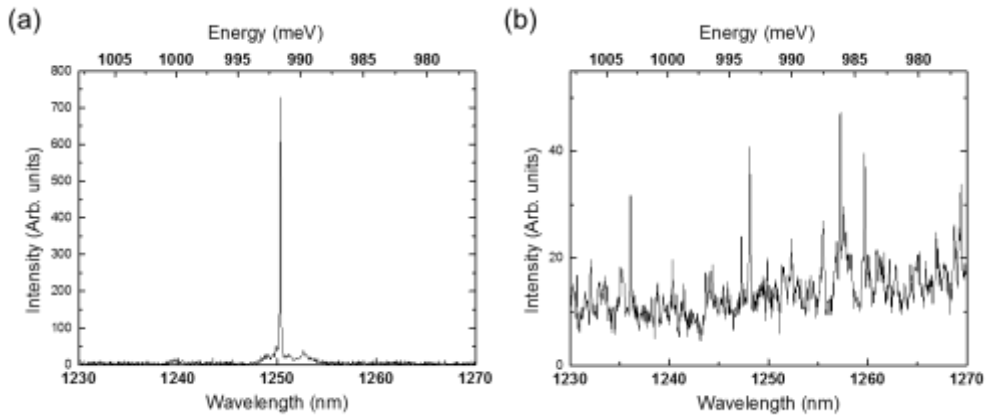

Figure S1. Photoluminescence spectra of (a) cavity-coupled dots and (b) bulk dots.

Comparison of lifetimes of bulk dots and cavity-coupled dots

Photonic crystal cavities can modify the local density of optical modes, resulting in enhancement or suppression of a spontaneous emission rate of dots. Figure S2 shows lifetimes of dots A and B, along with a bulk dot. Dots A and B show lifetimes of 1.12 ns and 1.06 ns respectively, which are shorter than the lifetime of a bulk InAs/InP dot of 1.9 ns. The bulk dots have the averaged lifetime of 1.78±0.2 ns. We also measure the lifetime of a dot in the cavity whose emission is spectrally detuned by 5 nm from the cavity mode. The off-resonant dot shows a slow lifetime of 2.9 ns, which is much longer than that of bulk dots. For spectrally detuned dots more than 5 nm they have the averaged lifetime of 3.2±0.8 ns.

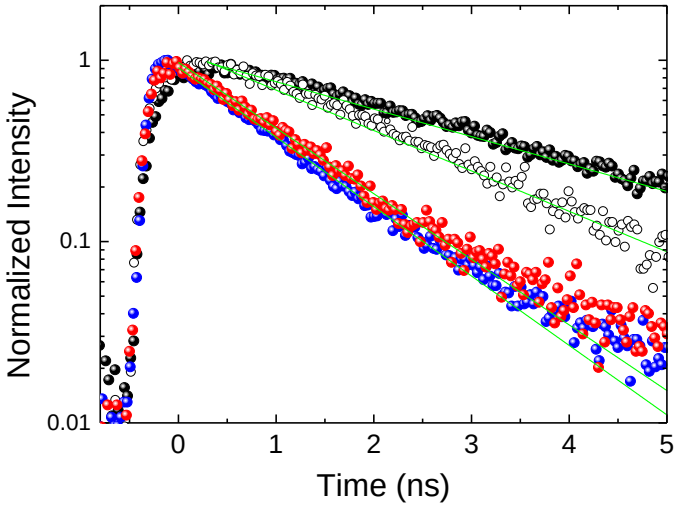

Figure S2. Lifetimes of the cavity-coupled dots A (red dots) and B (blue dots), an off-resonant dot (black dots), and a bulk dot (black open dots). Measured data are fitted by single exponential decay functions (green lines).

Polarization analysis of cavity-coupled dots

*L*3 photonic crystal cavity modes have strong polarization dependence which induces a linearly polarized emission of cavity-coupled dots.[2] Figure S3 shows a polar plot of the emission intensity of dots A and B. The polar plots show strong linear polarization ratios of 0.96±0.01 and 0.93±0.01 for dots A and B respectively. Dots A and B also show orthogonal polarized emission along the polarization axis of the cavity mode it is coupled to.

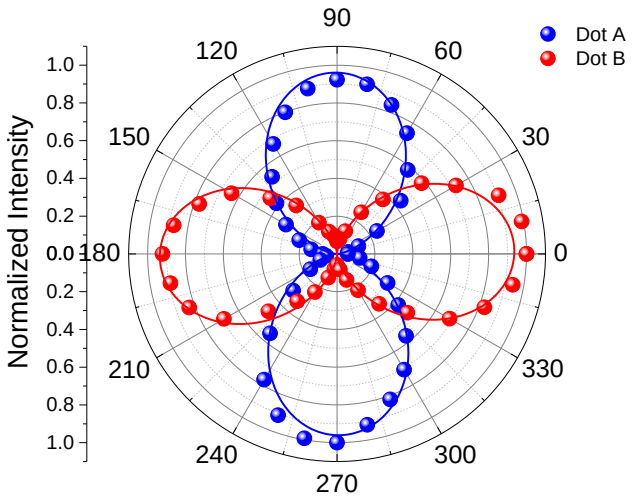

Figure S3. Polar plots of the single photon emission from dots A (blue dots) and B (red dots) as a function of polarization angle.

Influence of thermal tuning on second-order autocorrelation curves

Figure S4a shows the combined spectrum of dots A and B before thermal tuning (black line) and after thermal tuning (red line). In the presence of the heating laser we observe an increased broadband background contribution which we attribute to the other dots and/or nonresonantly coupled cavity emissions[3] excited beyond the tightly focused excitation. To estimate the background emission, we measure the photon counts at the dot emissions (S) and compare the values to the photon counts at 1 nm detuned wavelength (B) after thermal tuning, which give a ratio of quantum dot signal to total signal, $\rho_{A,B} = \frac{S_{A,B} - B_{A,B}}{S_{A,B}}$=0.91 and 0.94 for dots A and B respectively. This additional background emission degrades the $g^{(2)}(0)$ as shown in Figure S4b,c. These figures plot the second order correlation of dots A and B under continuous wave excitation. The anti-bunching we attain is worse than the value obtained under pulsed excitation (Figure 2d,e) due to the contribution of this background noise, and also to the finite time resolution of the detector. We fit the measured second-order correlation curves ($g^{(2)}_{A,B}(t)$) for dots A and B to the functions of $g^{(2)}_{A,B}(t) = 1 - (1 - g^{(2)}_{A,B}(0))e^{-\frac{|t|}{\tau_{A,B}}}$, where τ_A and τ_B are fitted parameters for the lifetime of each dot. To account for the finite time resolution of the detector, we convolve the second-order correlations functions with a Gaussian points spread function of 200 ps. The fitted curves show $g^{(2)}_A(0)$=0.43 and $g^{(2)}_B(0)$=0.45, indicating that the heating laser contributes background to both dots.

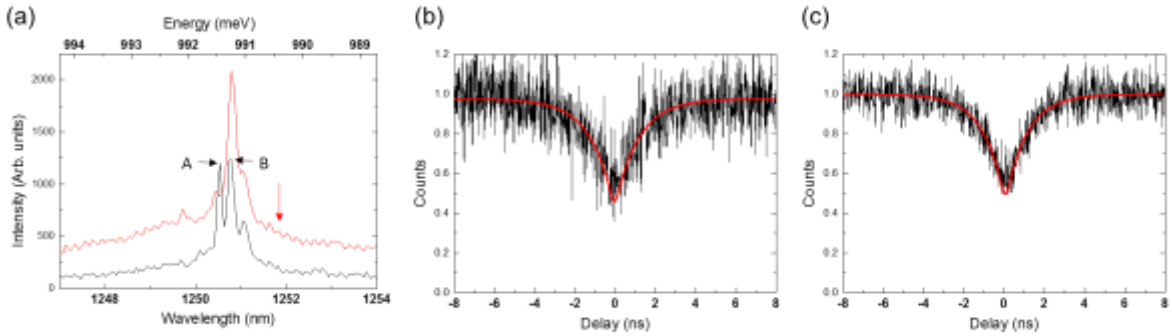

Figure S4. (a) Photoluminescence spectra of dots A and B before thermal tuning (black line) and after thermal tuning (red line). Black and red arrows denote dots A and B and the 1 nm detuned wavelength from the dot emissions to measure background counts. (b,c) Second-order autocorrelation curves of (b) dot A and (c) dot B. Red lines represent fitted curves.

Theoretical model for two-photon interference measurements

In contrast to a conventional Hong-Ou-Mandel experiments that measure the coincidence counts when two photons leave at the opposite sides of a 50:50 beamsplitter, our modified Hong-Ou-Mandel scheme measures the coincidence counts when two photons leave at the same side of a 50:50 beamsplitter. The second order correlation functions for the two-photon interference effect between two emitters with orthogonal ($g_{\perp}^{(2)}(t)$) and parallel ($g_{\parallel}^{(2)}(t)$) polarized photons are given by[4-6]

$$g_{\perp}^{(2)}(t) = \frac{g_A^{(2)}(t)+g_B^{(2)}(t)+2}{4} \quad (1)$$

$$g_{\parallel}^{(2)}(t) = \frac{g_A^{(2)}(t)+g_B^{(2)}(t)+2\left(1+V\rho_A\rho_B e^{-\frac{2|t|}{\tau_c}}\right)}{4} \quad (2)$$

where $g_{A,B}^{(2)}(t)$ and $\rho_{A,B} = 1 - \frac{B_{A,B}}{S_{A,B}}$ are the second-order auto-correlation and the ratio of the sample signal to total signal of dots A and B. V and τ_c are fitted parameters denoting the wavefunction overlap of two photons and the coherence time of dots A and B. The first two terms in eq 1,2 represent the probability of coincident counts due to multi photon events of the source itself or background emission, while the third term describes the probability of coincident counts originating from two-photon interference between two photons from opposite inputs of the beam splitter. The sources show a negligible detuning ($\Delta\omega \sim 0$), and we balance the emission intensities of two dots. We insert the measured $g_{A,B}^{(2)}(t)$ and $\rho_{A,B}$ for dots A and B, obtained from the previous section to eq 1,2, and convolve these equations with a Gaussian function that accounts for the limited time resolution of the detectors. With fitted parameters of V=0.96 and τ_c=115 ps, eq 1,2 fit the measured data in Figure 4 well.

References

(1) Barnes, W.; Björk, G.; Gérard, J.; Jonsson, P.; Wasey, J.; Worthing, P.; Zwiller, V. *Eur. Phys. J. D* **2002,** 18, 197-210.
(2) Kim, J.-H.; Cai, T.; Richardson, C. J. K.; Leavitt, R. P.; Waks, E. *Optica* **2016,** 3, 577-584.
(3) Majumdar, A.; Bajcsy, M.; Rundquist, A.; Kim, E.; Vučković, J. *Phys. Rev. B* **2012,** 85, 195301.
(4) Lettow, R.; Rezus, Y. L. A.; Renn, A.; Zumofen, G.; Ikonen, E.; Götzinger, S.; Sandoghdar, V. *Phys. Rev. Lett.* **2010,** 104, 123605.
(5) Stevenson, R. M.; Nilsson, J.; Bennett, A. J.; Skiba-Szymanska, J.; Farrer, I.; Ritchie, D. A.; Shields, A. J. *Nat. Commun.* **2013,** 4, 2859.
(6) Ou, Z.-Y. J., *Multi-photon quantum interference*; Springer: Berlin, 2007.